DOI: 10.3901/CJME.2016.0325.038, available online at www.springerlink.com; www.cjmenet.com

Simple PID Parameter Tuning Method Based on Outputs of the Closed Loop System

HAN Jianda[1], ZHU Zhiqiang[1, 2], JIANG Ziya[1, 2], and HE Yuqing[1, *]

1 *State Key Laboratory of Robotics, Shenyang Institute of Automation, Chinese Academy of Sciences, Shenyang 110016, China*
2 *University of Chinese Academy of Sciences, Beijing 100049, China*

Received September 15, 2015; revised January 7, 2016; accepted March 25, 2016

Abstract: Most of the existing PID parameters tuning methods are only effective with pre-known accurate system models, which often require some strict identification experiments and thus infeasible for many complicated systems. Actually, in most practical engineering applications, it is desirable for the PID tuning scheme to be directly based on the input-output response of the closed-loop system. Thus, a new parameter tuning scheme for PID controllers without explicit mathematical model is developed in this paper. The paper begins with a new frequency domain properties analysis of the PID controller. After that, the definition of characteristic frequency for the PID controller is given in order to study the mathematical relationship between the PID parameters and the open-loop frequency properties of the controlled system. Then, the concepts of M-field and θ-field are introduced, which are then used to explain how the PID control parameters influence the closed-loop frequency-magnitude property and its time responses. Subsequently, the new PID parameter tuning scheme, i.e., a group of tuning rules, is proposed based on the preceding analysis. Finally, both simulations and experiments are conducted, and the results verify the feasibility and validity of the proposed methods. This research proposes a PID parameter tuning method based on outputs of the closed loop system.

Keywords: PID control, characteristic frequency, step response, frequency property

1 Introduction

Owing to simple structure, the PID control has been widely applied in many real applications. Extensive theoretical studies have also been conducted on its parameter optimizing method. The well-known methods available in published literature include the Ziegler-Nichols method[1–2], the IMC method[3–5], and the loop-shaping method[6–7]. Unfortunately, these methods often require highly accurate system models, which necessitates time-consuming experiments for system identification in actual applications. Thus, the final closed loop performance will be certainly affected by the model inaccuracy. Although some robust design methods can be used to partly solve the problem, they can not be used extensively due to the often accompanied performance deterioration in the aspects of both servo tracking and disturbance suppression.

In practical engineering applications, it is desirable for the PID tuning rules to be directly based on the input-output data of the closed-loop system[8–11]. It is also preferable for the tuning rules to be as simple and easy as possible[12–13]. Thus in this paper, a new PID tuning strategy is proposed. The major advantage of the proposed method is that the problem of model uncertainty associated with system identification is avoided because model information of the controlled system are not explicitly required.

The steady, response speed and the disturbance rejection capacity are some main performance to be considered during the design of a PID controller[14–16]. In model based scheme, the trade-offs among them are made through elaborate analysis and calculations. However, in our study, the main concerns are to develop tuning method that is independent of model information and simple to apply. Thus, the trade-offs among the different criteria are realized based on detailed analysis of the PID control structure and its influences to both the time domain and frequency domain characteristics of the closed loop system.

The contents of this paper are organized as follows. In section 2, the frequency properties of the PID control structure are analyzed in detail. In section 3, the concepts of M-field and θ-field are introduced and analyzed to develop the relationship between the frequency properties of the open-loop system and those of the corresponding closed-loop system. Based on these results, the tuning rules are given and explained in section 4. Then, the simulations and experiments are conducted in section 5 to verify the effectiveness of the proposed tuning rules. Finally,

* Corresponding author. E-mail: heyuqing@sia.cn
Supported by National Natural Science Foundation of China (Grant Nos. 61473282, 61203340, 61305120)

concluding remarks are made in section 6.

2 Phase and Magnitude Analysis

A PID controller are of the frequency domain form $C(s)=K_p+K_i/s+K_d s$, and the phase and the magnitude at frequency ω are

$$\begin{cases} \arg C(j\omega) = \arctan\left(\left(K_d\omega - \frac{K_i}{\omega}\right)/K_p\right), \\ |C(j\omega)| = \sqrt{K_p{}^2 + \left(K_d\omega - \frac{K_i}{\omega}\right)^2}. \end{cases} \tag{1}$$

Using Eq. (1), the influence of K_p, K_i, K_d on the phase and magnitude of the PID controller can be given in the form of partial derivative functions as follows:

$$\begin{cases} \frac{\partial \arg C(j\omega)}{\partial K_p} = \left(\frac{K_i}{\omega} - K_d\omega\right)/|C(j\omega)|^2, \\ \frac{\partial |C(j\omega)|}{\partial K_p} = \frac{K_p}{|C(j\omega)|}, \end{cases} \tag{2}$$

$$\begin{cases} \frac{\partial \arg C(j\omega)}{\partial K_i} = \frac{-K_p}{\omega|C(j\omega)|^2}, \\ \frac{\partial |C(j\omega)|}{\partial K_i} = \left(\frac{K_i}{\omega} - K_d\omega\right)/(\omega|C(j\omega)|), \end{cases} \tag{3}$$

$$\begin{cases} \frac{\partial \arg C(j\omega)}{\partial K_d} = \frac{K_p\omega}{|C(j\omega)|^2}, \\ \frac{\partial |C(j\omega)|}{\partial K_d} = \frac{K_d\omega^2 - K_i}{|C(j\omega)|}. \end{cases} \tag{4}$$

From Eqs. (2)–(4), we can obtain the following equations:

$$\begin{cases} \frac{\partial \arg C(j\omega)}{\partial K_p} > 0, \quad \omega < \sqrt{\frac{K_i}{K_d}}, \\ \frac{\partial \arg C(j\omega)}{\partial K_p} < 0, \quad \omega > \sqrt{\frac{K_i}{K_d}}, \\ \frac{\partial |C(j\omega)|}{\partial K_p} > 0, \end{cases} \tag{5}$$

$$\begin{cases} \frac{\partial |C(j\omega)|}{\partial K_i} > 0, \quad \omega < \sqrt{\frac{K_i}{K_d}}, \\ \frac{\partial |C(j\omega)|}{\partial K_i} < 0, \quad \omega > \sqrt{\frac{K_i}{K_d}}, \\ \frac{\partial \arg C(j\omega)}{\partial K_i} < 0, \end{cases} \tag{6}$$

$$\begin{cases} \frac{\partial |C(j\omega)|}{\partial K_d} < 0, \quad \omega < \sqrt{\frac{K_i}{K_d}}, \\ \frac{\partial |C(j\omega)|}{\partial K_d} > 0, \quad \omega > \sqrt{\frac{K_i}{K_d}}, \\ \frac{\partial \arg C(j\omega)}{\partial K_d} > 0. \end{cases} \tag{7}$$

From Eq. (5)–Eq. (7), it can be seen that the term $\sqrt{K_i/K_d}$ is important in describing the phase and magnitude characteristics of the PID controller. Thus in the following discussions, $\omega_c = \sqrt{K_i/K_d}$ is defined as the characteristic frequency of the PID controller.

From Eqs. (3) and (4), we can also obtain the following relationships:

$$\left|\frac{\partial \arg C(j\omega)}{\partial K_i} \middle/ \frac{\partial \arg C(j\omega)}{\partial K_d}\right| = \frac{1}{\omega^2}, \tag{8}$$

$$\left|\frac{\partial |C(j\omega)|}{\partial K_i} \middle/ \frac{\partial |C(j\omega)|}{\partial K_d}\right| = \frac{1}{\omega^2}. \tag{9}$$

If $\omega < \omega_c$, from Eq. (8), we have,

$$\left|\frac{\partial \arg C(j\omega)}{\partial K_i} \middle/ \frac{\partial \arg C(j\omega)}{\partial K_d}\right| > \frac{1}{\omega_c^2} = \frac{K_d}{K_i}. \tag{10}$$

Hence

$$\left|\frac{\partial \arg C(j\omega)}{\partial \ln K_i}\right| > \left|\frac{\partial \arg C(j\omega)}{\partial \ln K_d}\right|, \omega < \omega_c. \tag{11}$$

Similarly, from Eq. (9) we have,

$$\left|\frac{\partial |C(j\omega)|}{\partial \ln K_i}\right| > \left|\frac{\partial |C(j\omega)|}{\partial \ln K_d}\right|, \omega < \omega_c. \tag{12}$$

When $\omega > \omega_c$, from Eqs. (8) and (9), we have

$$\begin{cases} \left|\frac{\partial \arg C(j\omega)}{\partial \ln K_i}\right| < \left|\frac{\partial \arg C(j\omega)}{\partial \ln K_d}\right|, \omega > \omega_c, \\ \left|\frac{\partial |C(j\omega)|}{\partial \ln K_i}\right| < \left|\frac{\partial |C(j\omega)|}{\partial \ln K_d}\right|, \omega > \omega_c. \end{cases} \tag{13}$$

Based on Eqs. (11)–(13), we can conclude that in order to enlarge or reduce the phase or the magnitude of PID controller at frequency ω, parameter $K_i\,(K_d)$ should be firstly regulated if $\omega < \omega_c\,(\omega > \omega_c)$.

3 M-filed and θ-field

The M-circle[18–21], defined as Eq. (14), is useful in determining the magnitude of the closed loop system based on the open loop transfer function:

$$\left(X+\frac{M^2}{M^2-1}\right)^2+Y^2=\frac{M^2}{(M^2-1)^2}. \quad (14)$$

The circle given in Eq. (14) is centered at $(-M^2/(M^2-1),\ 0)$, with the radius equal to $M/(M^2-1)$. For an open loop system $G(s)$ and a frequency ω, if

$$G(j\omega)=X+jY,$$

where X and Y are the same as that in Eq. (14). Suppose

$$H(s)=\frac{G(s)}{1+G(s)},$$

then

$$|H(j\omega)|=M.$$

For the convenient of discussion, we define M_m as a M-circle given by Eq. (14) with $M = m$. Specially, M_1 is the straight line $X = -0.5$.

According to Eq. (14), each point in the complex plane (excluding $-1+0 \cdot j$) is on the border of a unique M-circle. Thus we can build a scalar field $M(x, y)$, called M-field. The domain of M-field is the whole complex plane excluding $-1 + 0 \cdot j$.

The scalar field $M(x, y)$ is C^∞ continuous in its domain, so we can define its gradient vector field $\boldsymbol{V}(x,y)$.

The norm and direction of $\boldsymbol{V}(x,y)$ are respectively denoted as $V(x,y)$ and $\boldsymbol{v}(x,y)$. A lemma concerning the direction of $\boldsymbol{V}(x,y)$ is given in Appendix A. For M-circle, we have the following theorem.

Theorem 1. Given a point P in the domain of M-field, suppose the center of the M-circle passing through P is O'. Let $\angle O'PO=\theta$, the value of the M-field at P be $M(P)$, and the gradient vector of M-field at P be $\boldsymbol{V}(P)$, that is, $\boldsymbol{V}(P)=V(P)\cdot\boldsymbol{v}(P)$. Define the angle between the OP and the positive direction of X axis be $\phi\ (0\leqslant\phi\leqslant\pi)$, then we have the following conclusions:

$$\frac{\partial M(P)}{\partial|OP|}=-V(P)\cdot\cos\theta, \quad (15)$$

$$\frac{\partial M(P)}{\partial\phi}=V(P)\cdot|OP|\cdot\sin\theta. \quad (16)$$

Proof: Consider the case of $M(P) > 1$ as shown in Fig. 1. Suppose $\boldsymbol{a}$ and $\boldsymbol{b}$ are two unit direction vectors where $\boldsymbol{a}$ points from O to P and $\boldsymbol{b}$ is vertical to OP, then ϕ keeps increasing when P moves along the direction of $\boldsymbol{b}$.

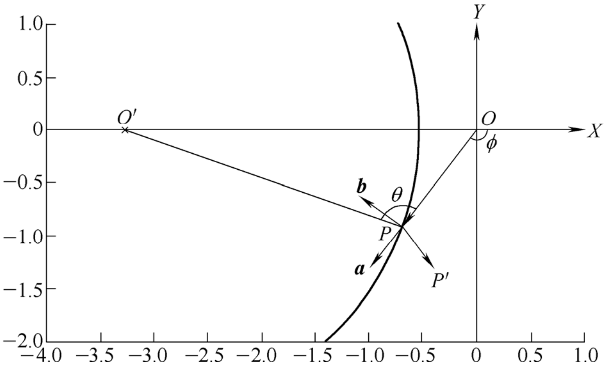

Fig. 1. Figure for theorem 1

Suppose P' is a point different from P and $|PP'|$ is infinitely small, A and B are the projections of $\overrightarrow{PP'}$ on $\boldsymbol{a}$ and $\boldsymbol{b}$, respectively. We have

$$\delta|OP|=|OP'|-|OP|=A, \quad (17)$$

$$\delta\phi=\angle POP'=\frac{B}{|OP|}. \quad (18)$$

As $|PP'|$ is infinitely small, the variation of $\boldsymbol{V}(x,y)$ can be neglected when $x+jy$ is moved from P to P'.

$$\delta M=M(P')-M(P)=\boldsymbol{V}(P)\cdot\overrightarrow{PP'}=\boldsymbol{V}(P)\cdot A\cdot\boldsymbol{a}+\boldsymbol{V}(P)\cdot B\cdot\boldsymbol{b}. \quad (19)$$

According to Lemma 1 (Appendix A), $\boldsymbol{V}(P)$ points from P to O', thus we have

$$\delta M=-V(P)\cdot\cos\theta\cdot A+V(P)\cdot\sin\theta\cdot B=-V(P)\cdot\cos\theta\cdot\delta|OP|+V(P)\cdot\sin\theta\cdot|OP|\cdot\delta\phi. \quad (20)$$

In differential form, Eq. (20) can be rewritten as

$$\mathrm{d}M=-V(P)\cdot\cos\theta\cdot\mathrm{d}|OP|+V(P)\cdot\sin\theta\cdot|OP|\cdot\mathrm{d}\phi. \quad (21)$$

Thus Eqs. (15) and (16) are proved for the case of $M(P)>1$.

In the similar way, it can be proved that when $M(P)<1$, Eqs. (15) and (16) still hold. This complete the proof of Theorem 1.

For a control system, suppose: 1) the value of the closed loop magnitude at ω is $M(j\omega)$, 2) the open loop transfer function $G(s)$ at ω can be denoted as $G(j\omega)=x+jy$, and 3) the point in the complex plane corresponding to $G(j\omega)$ is $P(x,y)$. Then $|G(j\omega)|=|OP|$, and $\arg G(j\omega)$ corresponds to the value of the angle between the positive direction of X axis and OP'. Theorem 1 tells us how $|G(j\omega)|$ and $\arg G(j\omega)$ influence $M(j\omega)$.

From Eqs. (15) and (16), we can see that θ plays an important role in determining both $\partial M(P)/\partial|OP|$ and $\partial M(P)/\partial\phi$. As a result, before introducing PID parameter tuning rules, we firstly analyze the value of θ at different points in the complex plane, and the results are given in the following Theorem 2.

Theorem 2. Given a point P in the domain of M-field. Suppose the M-circle passing through P is M_m, with $m \neq 1$. Let the center of M_m be O', and point $U = -1 + j \cdot 0$. We have

$$\angle O'PO = \theta \ (\theta \in [0, \pi]) \Leftrightarrow \angle PUO = \bar{\theta}, \tag{22}$$

where

$$\bar{\theta} = \begin{cases} \pi - \theta, & m > 1, \\ \theta, & m < 1. \end{cases}$$

Proof: Let the coordinate of P in complex plane be (X, Y). When $\angle O'PO = \theta$, according to the equation of M_m and the cosine theorem, we have

$$\left(X + \frac{m^2}{m^2 - 1}\right)^2 + Y^2 = \frac{m^2}{(m^2 - 1)^2}, \tag{23}$$

$$\frac{\left(X + \dfrac{m^2}{m^2 - 1}\right)^2 + X^2 + 2Y^2 - \dfrac{m^4}{(m^2 - 1)^2}}{2\sqrt{\left(X + \dfrac{m^2}{m^2 - 1}\right)^2 + Y^2} \cdot \sqrt{X^2 + Y^2}} = \cos\theta. \tag{24}$$

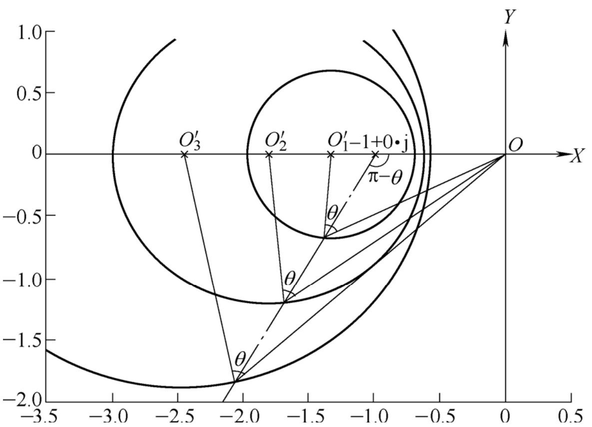

Fig. 2. An example for theorem 2

From Eq. (23), the following equation is satisfied,

$$X^2 + Y^2 = -\frac{m^2}{m^2 - 1}(2X + 1). \tag{25}$$

Substitute Eqs. (23) and (25) into Eq. (24), we have

$$(1 - m^2)(X + 1)^2 = (2X + 1)(\cos\theta)^2. \tag{26}$$

Substitute Eq. (23) into Eq. (24), and substitute Eq. (25) into Eq. (24):

$$m^2 (X + 1)^2 = (X^2 + Y^2)(\cos\theta)^2. \tag{27}$$

Furthermore, substitute Eq. (26) into Eq. (27):

$$(X + 1)^2 = (X^2 + 2X + 1 + Y^2)(\cos\theta)^2. \tag{28}$$

Hence

$$(1 - (\cos\theta)^2)(X + 1)^2 = Y^2 (\cos\theta)^2. \tag{29}$$

Thus, if $(X, Y) \neq (-1, 0)$, $\theta = \pi/2 \Leftrightarrow X = -1$. That means, $\theta = \pi/2$ is equivalent to P is on the line $X = -1$, as shown in Fig. 3.

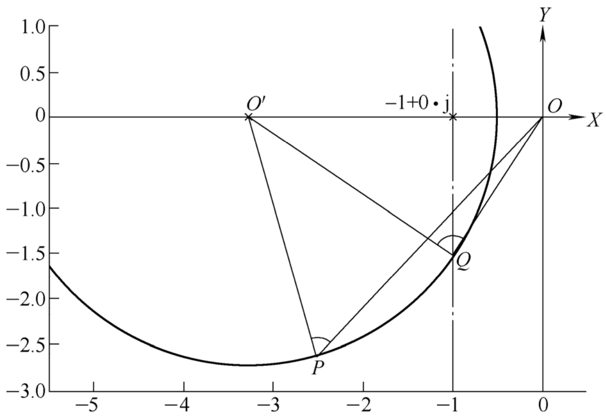

Fig. 3. Value of θ in t he domain of M-field

If $(X, Y) \neq (-1, 0)$ and $\theta \neq \pi/2$, we have

$$\tan\angle PUO = \frac{Y}{X + 1} = \pm\tan\theta. \tag{30}$$

That is, $\bar{\theta} = \angle PUO = \theta$ or $\bar{\theta} = \angle PUO = \pi - \theta$.

Let P and Q be any two points in M_m (as shown in Fig. 3). Q is on the line $X = -1$ (which means $\angle QUO = \pi/2$, $\angle OQO' = \pi/2$).

If P is on the left side of the line $X = -1$, it is easy to show that $|OP| > |OQ|$. According to the cosine theorem, $\theta = \angle OPO' < \angle OQO' = \pi/2$. However, it is obvious that $\bar{\theta} = \angle OUP > \pi/2$.

On the other hand, if P is on the right side of the line $X = -1$, then $\theta = \angle O'PO > \pi/2$ and $\bar{\theta} = \angle PUO < \pi/2$.

So we can conclude that if $m > 1$, then $\bar{\theta} = \pi - \theta$.

When $m < 1$, $\bar{\theta} = \angle PUO < \pi/2$, as O is inside M_m, $\theta = \angle O'PO < \pi/2$. So $\bar{\theta} = \theta$.

Thus Theorem 2 is proved.

According to Theorem 2, given a point P in the complex plane with coordinate $(X, Y) \notin \{(0,0), (-1,0)\}$, there is a unique value of θ corresponding to P. Thus we can define a scalar field $\theta(X, Y)$, named θ-field, shown as Fig. 4.

θ-field is useful in determining how $|G(j\omega)|$ and $\arg G(j\omega)$ influence $M(j\omega)$. For example, if $G(j\omega)$ is in the line segment of UO, then $\theta(G(j\omega)) = \pi$, according to Eqs. (15) and (16), $M(j\omega)$ increases if $|G(j\omega)|$ increases, while $\arg G(j\omega)$ has no influence on $M(j\omega)$; if $G(j\omega)$ is in the line segment of $X = -1 (Y \neq 0)$, then

$\theta(G(j\omega))=\pi/2$, $M(j\omega)$ decreases if $\arg G(j\omega)$ increases, while $|G(j\omega)|$ has no influence on $M(j\omega)$.

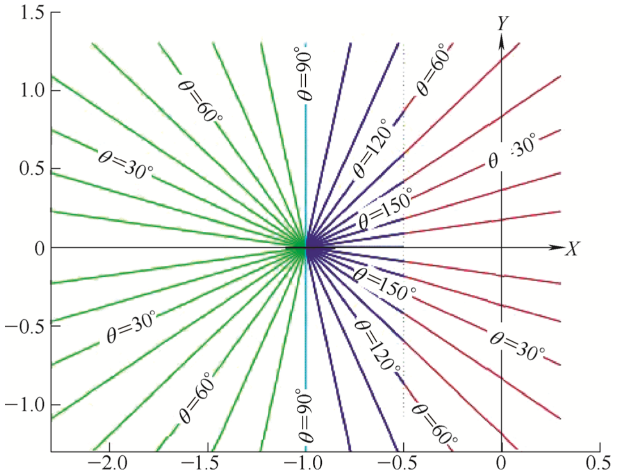

Fig. 4. θ-field

Using the θ-field, the complex plane can be divided into the following three parts.

Part I: $\{X+jY \mid X\leqslant -1, X+jY\neq -1, X\in R, Y\in R\}$, in this part, $\theta\leqslant\pi/2$.

Part II: $\{X+jY \mid -1<X<-0.5, X\in R, Y\in R\}$, in this part, $\pi/2<\theta\leqslant\pi$.

Part III: $\{X+jY \mid X\geqslant -0.5, X+jY\neq 0, X\in R, Y\in R\}$, in this part, $\theta\leqslant\pi/2$.

4 Tuning Method

In real applications, there are several main requirements of the dynamical characteristics of PID control system: the first one is the steady, i.e., the oscillation in step response should be as low as possible; the second one is the response speed, i.e., the system should get to the desired set point as quick as possible; and the third one is the disturbance attenuation performance, i.e., the system should be insensitive to the external disturbances. The proposed method of this paper is based on a balance of these requirements. The whole tuning process is composed of two main sub-steps: The first one is to regulate the parameters based on the preceding analysis to reduce the oscillation, and the second one is to enlarge the parameter, especially the proportion gain K_p, to improve the disturbance attenuation capacity and response speed.

In this section, we will mainly discuss how to reduce the oscillation in system response, and a set of PID parameter tuning rules are proposed based on the preceding results.

Suppose the frequency of the oscillation in the PID control system output is ω_o. ω_o can be roughly measured in the way shown in the lower figure of Fig. 5. In fact, ω_o can also be obtained through frequency domain analysis algorithm, i.e., FFT. The open loop transfer function of the system is:

$$G(s)=(4+12/s+0.2s)\exp(-0.1s)/(1+s).$$

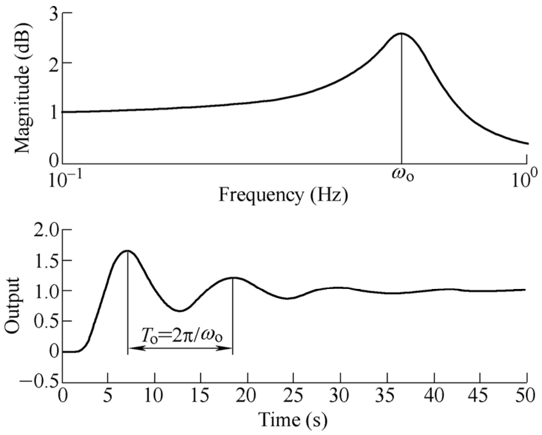

Fig. 5. The closed loop magnitude and step response

Suppose $H(s)$ is the transfer function of the closed loop system. That is, $H(s)=G(s)/(1+G(s))$. In order to attenuate the oscillation of the closed loop response, one of the effective scheme is to reduce $|H(\omega)|$ in the frequency section around ω_o through regulating properly the controller parameters.

Before the discussion on how to reduce the oscillation, we should firstly study the position of $G(j\omega_o)$ in the θ-field, which is important for determining the parameter tuning rules. Three facts are given as follows:

First: if the point corresponding to $G(j\omega)$ is in part III in the θ-field, then $|H(j\omega)|<1$, so $G(j\omega_o)$ can't be in part III of the θ-field.

Second: for most actual control system, the open loop transfer function presents low pass characteristic. That is, as ω increases, both $|G(j\omega)|$ and $\arg G(j\omega)$ decreases. So, in the frequency section where $\arg G(j\omega)<-\pi$, $|G(j\omega)|$ should be much smaller than 1 (for a stable system). So, it is very rare that the phase of the open loop transfer function at the oscillation frequency ω_o is smaller than $-\pi$, which means that the position of $G(j\omega_o)$ in the complex plane should be under the real axis.

Third: if the point corresponding to $G(j\omega)$ is in part I of the θ-field ($\theta(G(j\omega))<\pi/2$), according to Eqs. (15) and (16) in Theorem 2, neither $|G(j\omega)|$ nor $\arg G(j\omega)$ can be regulated to increase $|H(\omega)|$. On the other hand, both $G(j\omega)$ and $\arg G(j\omega)$ decrease as ω increases in this domain (low pass characteristic of $G(j\omega)$). As a result, $G(j\omega_o)$ can't be in part I of the θ-field.

Based on the above three facts, the following assumption is given,

Assumption 1. $G(j\omega_o)$ is in Part II of the θ-field ($\pi/2<\theta(G(j\omega_o))<\pi$) and is under the real axis.

With Assumption 1, the PID parameter tuning rules can be designed as follows,

Case 1: low frequency oscillation ($\omega_o<\omega_c$).

Considering Eqs. (15) and (16), the variation of K_d is less effective than that of K_i, so K_p or K_i should be adjusted. Furthermore, according to assumption 1 and Eq. (15)–Eq. (16) in Theorem 2, in order to decrease $|H(\omega_o)|$, we should decrease $|G(\omega_o)|$ and increase $\arg G(\omega_o)$. As $\omega<\omega_c$, according to Eq. (5)–Eq. (7) in section II, only decreasing K_i or increasing K_d can decrease $|G(\omega_o)|$ and increase $\arg G(\omega_o)$ at the same time. Considering Eqs. (11) and (12), we should decrease K_i to decrease $|H(\omega_o)|$ for this case.

However, there are two special conditions in case 1.

Special case 1-1: $G(j\omega_o)$ is close to the real axis. In this condition, $\theta(G(j\omega_o))$ is close to π. According to Eqs. (15) and (16) in Theorem 2, the variation of $\arg G(\omega_o)$ has little influence on $|H(\omega_o)|$, however, as decreasing $|G(\omega_o)|$ can decrease $|H(\omega_o)|$, decreasing K_i is still an effective tuning method.

Special case 1-2: $G(j\omega_o)$ is closed to the line $X=-1$. In this condition, $\theta(G(j\omega_o))$ is close to $\pi/2$. According to Eqs. (15) and (16) in Theorem 2, the variation of $|G(\omega_o)|$ has little influence on $|H(\omega_o)|$, and increasing $\arg G(j\omega_o)$ can decrease $|H(\omega_o)|$. As we want $|G(\omega_o)|$ to be as large as possible for the capacity of servo tracking and disturbance suppression, increasing K_p is a better tuning rule than decreasing K_i for this special condition.

Case 2: high frequency oscillation ($\omega_o > \omega_c$).

Considering Eq. (13), the variation of K_i is less effective than that of K_d, so K_p or K_d should be adjusted. Furthermore, similar to case 1, $|G(\omega_o)|$ should be decreased and $\arg G(\omega_o)$ should be increased to decrease $|H(\omega_o)|$. As $\omega > \omega_c$, only decreasing K_p can decrease $|G(\omega_o)|$ and increase $\arg G(j\omega_o)$ at the same time according to Eqs. (5)–(7) in section II. Thus the parameter tuning method for case 2 is to decrease K_p.

There are also two special conditions for case 2.

Special case 2-1: $G(j\omega_o)$ is closed to the real axis. As that in case 1, in this condition, the variation of $\arg G(\omega_o)$ has little influence on $|H(\omega_o)|$, and decreasing $|G(\omega_o)|$ can decrease $|H(\omega_o)|$. As both decreasing K_p and decreasing K_d can decrease $|G(\omega_o)|$, and decreasing K_p leads to the decreasing of $|G(\omega)|$ in frequency section where $\omega < \omega_c$ (which weakens the capacity of servo tracking and disturbance suppression). Thus, in this special condition, decreasing K_d is a better method.

Special case 2-2: $G(j\omega_o)$ is close to the line $X=-1$. As that in case 1, the variation of $|G(\omega_o)|$ has little influence on $|H(\omega_o)|$, and increasing $\arg G(j\omega_o)$ can decrease $|H(\omega_o)|$. So we should decrease K_p or increase K_d. Suppose ω_u is the frequency, s.t., $\arg G(\omega_u) = -\pi$, as ω_u is a high frequency ($\omega_c < \omega_o < \omega_u$), increasing K_d can lead to the increasing of $|G(\omega_u)|$. As $\theta(G(j\omega_u)) = \pi$, $|H(\omega_u)|$ is very sensitive to $|G(\omega_u)|$. Thus in this condition, we should decrease K_p.

In conclusion, the tuning rules are summarized in the following Table 1.

Remark I: In real applications, it is difficult to distinguish whether the system fulfils the special condition or not based only on the system response. However, for each case, there are only one special condition that requires a different tuning method, so for each case, the tuning methods can be selected by trial and error directly.

Table 1. Methods of alleviating system oscillation

Cases	Tuning methods
Case 1 ($\omega_0 < \omega_c$)	Decreasing K_i Increasing K_p *
Case 2 ($\omega_0 > \omega_c$)	Decreasing K_p Decreasing K_d **

Note: * If $G(j\omega_o)$ is close to line $X=-1$.
** If $G(j\omega_o)$ is close to the real axis.

Remark II: Generally, we want the magnitude of the open loop transfer function to be as large as possible due to the requirements of disturbance suppression and servo tracking. Thus, for case 1, increasing K_p should be tried first. In case 2, as decreasing K_p can reduce the magnitude of the open loop transfer function in the low frequency section, thus weakens the capacity of disturbance suppression, so decreasing K_d should be tried first.

A flow chart of PID parameter tuning procedure is given in Fig. 6, where decrease (increase) a parameter, means gradually decrease (increase) it until the oscillation disappears or the decreasing (increasing) of this parameter can no longer reduce the oscillation.

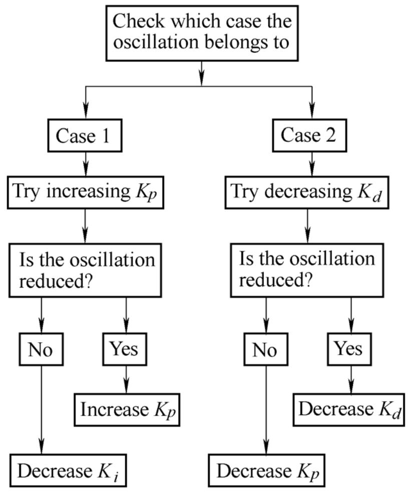

Fig. 6. Flow chart of tuning method

The tuning procedure shown in Fig. 6 tells which parameter should be regulated (increased or decreased), but there can be cases that the parameters are over tuned. To solve this problem, multi-round tuning strategy is proposed, shown in Fig. 7.

In Fig. 7, the steps enclosed in the thick line constitute one round of tuning. Suppose K_p^i, K_i^i and K_d^i are the values of K_p, K_i and K_d after the ith round of tuning. δ is defined as follows:

$$\delta^i = \left|\frac{K_p^i - K_p^{i-1}}{K_p^i}\right| + \left|\frac{K_i^i - K_i^{i-1}}{K_i^i}\right| + \left|\frac{K_d^i - K_d^{i-1}}{K_d^i}\right|, \quad (31)$$

where δ_0 is a pre-defined positive number. If the results of current round and the last round fulfills the inequality in the box, then the variation of parameters would be very small if tuning continues, so the tuning procedure can be stopped. With a smaller δ_0, the difference between the resulted PID controller and the ideal one would be smaller. So the value of δ_0 depends on the requirement of the performance of the resulted system and the number of tuning rounds that is acceptable.

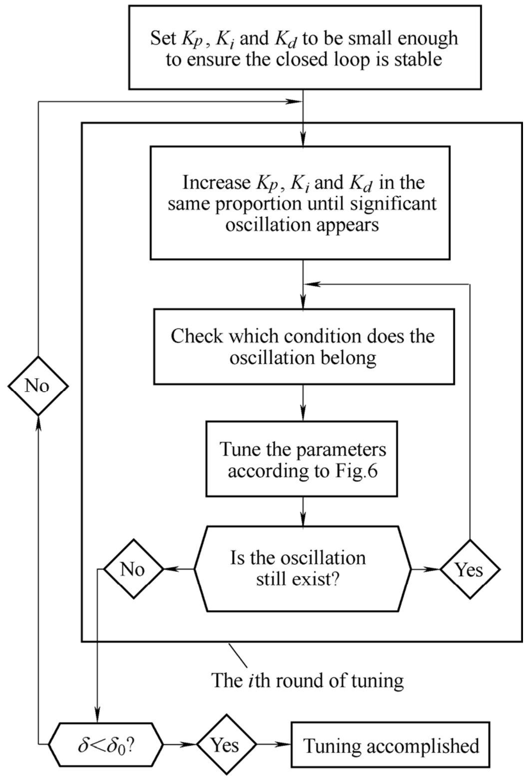

Fig. 7. Flow chart of multi-round tuning strategy

In the actual application, a PID controller should contain a low pass filter as follows:

$$C(s)=K_p+\frac{K_i}{s}+\frac{K_d s}{1+\lambda s}, \tag{32}$$

where λ is determined according to the requirement of noise filtering.

To apply the magnitude and phase properties given in Eqs. (1) and (32) can be transformed as

$$C(s)=K_p+\frac{K_i}{s}+\frac{K_d s}{1+\lambda s}= \\ \frac{K_p s(1+\lambda s)+K_i(1+\lambda s)+K_d s^2}{s(1+\lambda s)}= \\ \frac{(K_p+K_i\lambda)+K_i/s+(K_d+K_p\lambda)s}{1+\lambda s}. \tag{33}$$

Define

$$K_p'=K_p+K_i\lambda, \\ K_d'=K_d+K_p\lambda, \\ C'(s)=K_p'+K_i/s+K_d's,$$

and we have:

$$C(s)=\frac{C'(s)}{1+\lambda s}.$$

It should be noted that the tuning method given in this paper doesn't need the model information of the controlled plant, so $1/(1+\lambda s)$ can be treated as a part of the plant and the tuning procedure can be remained unchanged.

Eq. (1) can be rewritten as:

$$\begin{cases} \arg C'(j\omega)=\arctan\left(\left(K_d'\omega-\dfrac{K_i}{\omega}\right)\Big/K_p'\right), \\ \left|C'(j\omega)\right|=\sqrt{K_p'^2+\left(K_d'\omega-\dfrac{K_i}{\omega}\right)^2}. \end{cases} \tag{34}$$

Thus the tuning method given in this paper can be applied based on Eq. (34). In this case, the characteristic frequency of the PID controller is defined as:

$$\omega_c'=\sqrt{\frac{K_i}{K_d'}}=\sqrt{\frac{K_i}{K_d+K_p\lambda}}. \tag{35}$$

5 Simulations and Experiments

In this section, the proposed PID parameter tuning method is verified through both simulations and real experiments.

5.1 Simulations

In the simulations, the proposed tuning method is applied on the plant from Ref. [17], with the transfer function given as:

$$G_{p1}(s)=\frac{(-0.3s+1)(0.08s+1)}{(2s+1)(s+1)(0.4s+1)(0.2s+1)(0.05s+1)^3}.$$

In Fig. 8, curves *a*–*q* show the system outputs in different tuning steps, and the corresponding PID parameters are given in Table 2. The stop value of δ_0 is 0.1.

From Fig. 8 and Table 2, in the second tuning step, increasing K_p is firstly tried, and oscillation in system output (shown as curve *c* in Fig. 8) is not reduced. So in the third tuning step, K_p is restored to 2 and then K_i is decreased.

There are totally 3 rounds of tuning procedure for this simulation. From curve *a* to curve *h* form the first round, and δ at the end of this round is 1.3. From curve *i* to curve *k* form the second round, and the final δ is 0.43. From curve l to curve n form the third round and δ is 1.5. If the PID parameters are increased again, it can be verified that the parameters would be tuned back to very close to the parameter settings corresponding to curve *n*. That is, δ would be very small (far smaller than δ_0=0.1). So the tuning procedure is stopped.

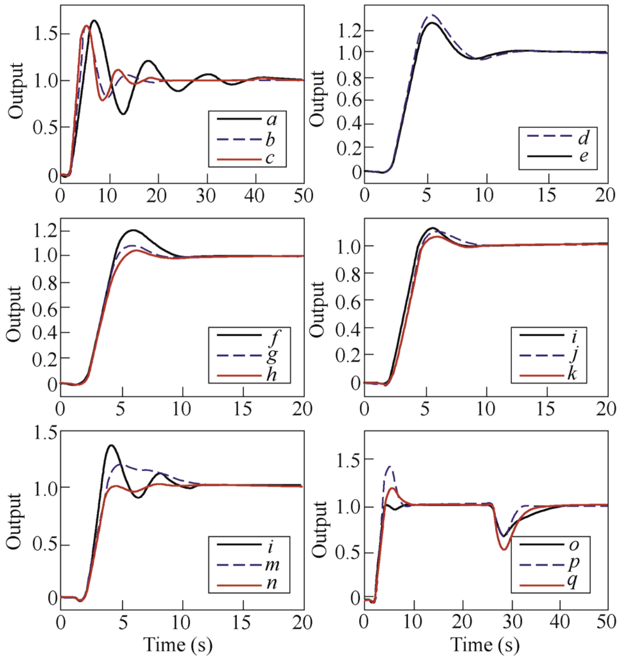

Fig. 8. Curves of simulation 1

Table 2. PID parameters in tuning steps of simulation

Curve	K_p	K_i	K_d	Case	Tuning method	δ
a	1	1	1	1	Increasing K_p	–
b	2	1	1	1	Increasing K_p	–
c	2.5	1	1	1	Restore parameter and decrease K_i	–
d	2	0.7	1	1	Decreasing K_i	–
e	2	0.6	1	2	Decreasing K_p	–
f	1.7	0.6	1	1	Decreasing K_i	–
g	1.7	0.45	1	1	Decreasing K_i	–
h	1.7	0.4	1	–	–	1.3
i	2	0.5	1.25	2	Decreasing K_p	–
j	1.8	0.5	1.25	1	Decreasing K_i	–
k	1.8	0.45	1.25	–	–	0.43
l	3.6	0.9	2.5	2	Decreasing K_p	–
m	2.5	0.9	2.5	1	Decreasing K_i	–
n	2.5	0.5	2.5	–	–	1.5

The final tuning result is compared with the tuning results of two well-known PID tuning methods. Curves *o*–*q* in Fig. 8 show the performance of set-point servo tracking and step disturbance suppression of PID control systems tuning by different methods: *o*-the Ziegler-Nichols method; *p*-the SIMC method[17]; *q*-the method given in this paper.

From these figures, it can be seen that the set-point servo tracking property of the system tuned by the proposed method is much better than that of the other two methods. As to the step disturbance suppression capacity, the system tuned by the proposed method is a little weaker than the Ziegler-Nichols method but is better than the SIMC method.

5.2 Experiments

Experiments are also applied on a rotating platform as shown in Fig. 9 to verify the priority of the proposed method. This platform is driven by a torque motor enclosed in the basement, and the rotating speed, which is the output in our experiments, is measured using a gyro, ADIS16135, produced by Analog Devices incorporation.

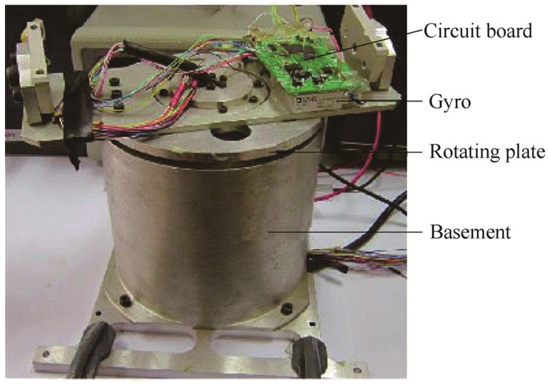

Fig. 9. Experimental rotating platform

All the parameter settings during the tuning process are listed out in Table 3, and Fig. 10 supplies curves of the most typical system output in the tuning process, which are from a to d. The stop value of δ_0 is given as 0.1.

Table 3. PID parameters in tuning steps of experiment

Curve	K_p	K_i	K_d	Case	Tuning method	δ
a, *b*	1.5	1.5	1.5	2	Decreasing K_d	–
b	1.5	1.5	1.2	2	Decreasing K_d	–
c	1.5	1.5	1	1	Increasing K_p	–
d	2	1.5	1	–	–	0.67
	2.67	2	1.3	2	Decreasing K_d	–
	2.67	2	1	1	Increasing K_p	–
	4	2	1	–	–	1
	6	3	1.5	2	Decreasing K_d	–
	6	3	1	–	–	1
	8	4	1.33	2	Decreasing K_d	–
	8	4	1	–	–	0.33
	10	5	1.25	2	Decreasing K_d	–
	10	5	1	–	–	0.25

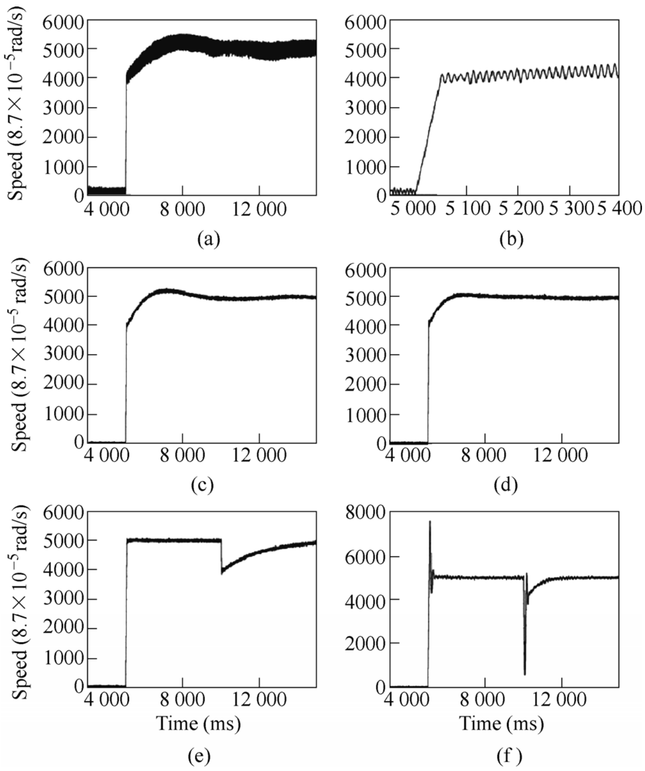

Fig. 10. Typical system outputs in the experiment 1

As given in Table 3, the initial setting for the PID controller is $G_k = 1.5 + 1.5/s + 1.5s$. Under these control parameters, the closed loop response is shown as Fig. 10(a), from which we can see that the high frequency oscillation appears, since $\omega_c = \sqrt{K_i / K_d} = 1$, we can directly conclude that $\omega_o > \omega_c$, thus from Fig. 6, decreasing K_d is conducted. After that, we can obtain a new closed loop response as shown in Fig. 10(b), and the same phenomenon appears thus we continue decreasing K_d and obtain the new closed loop as shown in Fig. 10(c). The tuning procedure is conducted until a good enough closed loop response is obtained (Table 3).

There are totally 5 rounds of tuning procedure. δ in these tuning rounds are respectively 0.67, 1, 1, 0.33, and 0.25. It can be verified that if another tuning round is carried out, then δ would be very small (far smaller than $\delta_0 = 0.1$). So the tuning procedure is stopped.

Fig. 10(e) and Fig. 10(f) give out the performance comparisons for different methods, where Fig. 10(e) is the result of the proposed method and Fig. 10(f) is the result of the Ziegler-Nichols method.

From these results, it can be seen that the set-point servo tracking property of the system by the proposed method is much better than that of the Ziegler-Nichols method. As to the step disturbance suppression, though the system output of proposed method has a longer recovering time, the fluctuation has a much smaller magnitude than that of the Ziegler-Nichols method.

6 Conclusions

In this paper, input-output responses based PID parameter tuning problem is researched. The main contributions of this paper are as following two aspects,

(1) A new kind of frequency domain analyzing method for PID control based on the concepts of M-filed and θ field is proposed.

(2) A set of PID parameter tuning rules are designed, whose main advantages are that only input-output step response data are required and the tuning procedure is easily implemented.

Simulations on an often referred-to dynamical system and experiments with respect to a real rotating platform driven by the motor are conducted. The detailed PID parameter tuning procedure are explained to show the validity of the proposed scheme. Furthermore, the final closed loop performance is compared to that based on some other PID parameter tuning scheme and the results show the priority of our proposed algorithm.

References

[1] ZIEGLER J G, NICHOLS N B. Optimum setting for automatic controllers[J]. *Transactions of ASME*, 1942, 64: 759–768.

[2] ASTROM K J, HAGLUND T. *PID controllers: Theory, design and tuning. Instrument Society of America*[M]. Research Trangle Park, NC, U.S.A. 1995.

[3] KWOK K E, PING M C, LI P. A model-based augmented PID algorithm[J]. *Journal of Process Control*, 2000, 10: 9–18.

[4] GOREZ R. New design relations for 2-DOF PID-like control system[J]. *Automatica*, 2003, 39: 901–908.

[5] MADHURANTHAKAM C R, ELKAMEL A, BUDMAN H. Optimal tuning of PID controllers for FOPTD, SOPTD and SOPTD with lead processes[J]. *Chemical Engineering and Processing*, 2008, 47: 251–264.

[6] SCHINSTOCK D E, ZHOU H W, TAO Y. Loop shaping design for tracking performance in machine axes[J]. *ISA Transactions*, 2006, 45: 5566.

[7] GRASSI E, TSAKALIS K. PID controller tuning by frequency loop shaping[C]//*Proceedings of the IEEE Conference on Decision and Control*, Japan, December 11–13, 1996: 4776–4781.

[8] UNBEHUAEN H, RAO G P. A review of identification in continuous-time systems[J]. *Annual Reviews in Control*, 1998, 22: 145–171.

[9] LIU T, GAO F. Closed-loop step response identification of integrating and unstable processes[J]. *Chemical Engineering Science*, 2010, 65: 2884–2895.

[10] ALI A, MAJHI S. PI/PID controller design based on IMC and percentage overshoot specification to controller set-point change[J]. *ISA Transactions*, 2009, 48: 10–15.

[11] PAVKOVIC D, POLAK S, ZORC D. PID controller auto-tuning based on process step response and damping optimum criterion[J]. *ISA Transactions*, 2014, 53(1): 85–96.

[12] ASTROM K J, HAGGLUND T. The future of PID control[J]. *Control Engineering Practice*, 2001, 9: 1163–1175.

[13] SHAMSUZZOHA M, SKOGESTAD S. The set-point overshoot method: A simple and fast closed-loop approach for PID tuning[J]. *Journal of Process Control*, 2010, 20: 1220–1234.

[14] ALCANTARA S, VILANOVA R, PEDRET C. PID control in terms of robustness/performance and servo/regulator trade-offs: A unifying approach to balanced auto-tuning[J]. *Journal of Process Control*, 2013, 23: 527–542.

[15] HUBA M. Performance measures, performance limits and optimal PI control for the IPDT plant[J]. *Journal of Process Control*, 2013, 23: 500–515.

[16] VERONESI M, VISIOLIA. Performance assessment and retuning of PID controllers[J]. *Industrial and Engineering Chemistry Research*, 2009, 48(5): 2616–2623.

[17] SKOGESTAD S. Simple analytic rules for model reduction and PID controller tuning[J]. *Journal of Process Control*, 2003, 13: 291–309.

[18] OGATA K. *Modern control engineering*[M]. 3rd ed. Prentice Hall. Upper Saddle River, NJ, USA. 2001.

[19] ISAAC M H. *Synthesis of feedback systems*[M]. Academic Press, 1963.

[20] BORIS J L, PAUL J E. *Classical feedback control*[M]. Marcel Dekker, 2000.

[21] STUBBERUD A, WILLIAMS I, DESTEFANO J. *Shaum's outline of feedback and control systems*[M]. McGraw-Hill, 1995.

Biographical notes

HAN Jianda, born in 1968, is currently a professor at *State Key Laboratory of Robotics, Shenyang Institute of Automation, Chinese Academy of Sciences*. His research interests include intelligent systems and robotics.
E-mail: jdhan@sia.cn

ZHU Zhiqiang, born in 1986, is currently a PhD candidate at *State Key Laboratory of Robotics, Shenyang Institute of Automation, Chinese Academy of Sciences*. His research interests include mechatronic systems design and vibration attenuating control.
Email: zhuzhiqiang@sia.cn

JIANG Ziya, born in 1988, is currently a PhD candidate at *State Key Laboratory of Robotics, Shenyang Institute of Automation, Chinese Academy of Sciences*. His research interests include nonlinear estimation and control of mobile robots.
E-mail: zyjiang@sia.cn

HE Yuqing, born in 1980, is currently a professor at *State Key Laboratory of Robotics, Shenyang Institute of Automation, Chinese Academy of Sciences*. His research interests include nonlinear systems and advanced control strategies.

Appendix A

Lemma 1. Given M_m, and a point $X+jY$ belonging to M_m, if $m>1\,(m<1)$, then gradient vector $\boldsymbol{V}(X,Y)$ points to the inside (outside) of M_m along the normal line of M_m at $X+jY$.

Proof:

Let ***t*** and ***n*** be the direction vector of the tangent line and the normal line of M_m at $X+jY$, T and N be the projections of $\boldsymbol{V}(X,Y)$ on ***t*** and ***n***. Then we have:

$$\boldsymbol{V}(X,Y)=T\bullet\boldsymbol{t}+N\bullet\boldsymbol{n}. \tag{A1}$$

According to the definition of M-circle, $M(x,y)$ is constant on M_m. Thus according to the definition of gradient vector, we have

$$\boldsymbol{V}(X,Y)\bullet\boldsymbol{t}=T=0. \tag{A2}$$

This means $\boldsymbol{V}(X,Y)=N\bullet\boldsymbol{n}$, and the following conclusions are obvious:

(1) When $m>1$, $M(X,Y)>m\Leftrightarrow X+jY$ is inside M_m;

(2) When $m<1$, $M(X,Y)>m\Leftrightarrow X+jY$ is outside M_m.